



Dynamic Tracking of Self-Healing Performance in Temperature-Sensitive Hydrogel Modified Asphalt Pavement Using Magnetic Resonance Imaging (MRI)

Yongjun Qiao¹, Mingji Li² and Fengwei Ma^{3,*}

¹ Shandong University Capital Operation Co., Ltd., Jinan 250100, Shandong, China

² Shandong HuaTe Road Materials Co., Ltd., Binzhou 251900, Shandong, China

³ Graduate School of Shandong University, Jinan 250100, Shandong, China

SUMMARY: *Traditional repair methods suffer from poor penetration and limited effectiveness. This study uses SK-70 base asphalt as the matrix, incorporating 5% N-isopropylacrylamide-based temperature-sensitive hydrogel with particle size of 50~80 micrometers, lower critical solution temperature of 33°C, and crosslinking degree of 0.45% to prepare modified asphalt. A 7.0T MRI system was employed to dynamically track the crack healing process, combined with three-point bending tests and rheological measurements to evaluate its self-healing and pavement performance. Experimental results show that when triggered at 40°C, the relative signal intensity ratio in the crack region increased rapidly from 0.32 at 0 min to 0.68 at 30 min, reaching 0.91 at 240 min, and stabilizing at 0.92~0.95 at 480 min, with cracks completely disappearing from MRI images. Macroscopic self-healing efficiency improved with healing time, reaching 38.5% at 2 h, 67.2% at 4 h, and 89.3% at 8 h. Rheological tests demonstrate that the complex modulus of modified asphalt exceeds that of base asphalt at 20~35°C, with the modulus decline rate slowing at the 33°C phase transition temperature, indicating superior pavement performance. MRI enables intuitive and precise tracking of the entire micro-crack healing process. Temperature-sensitive hydrogel modified asphalt, leveraging its temperature-responsive phase transition characteristics, can efficiently fill micro-cracks, providing a reliable microscopic characterization method and novel technical pathway for asphalt pavement self-healing technology.*

KEYWORDS: *temperature-sensitive hydrogel; modified asphalt; self-healing; magnetic resonance imaging; dynamic tracking*

1 Introduction

Asphalt pavement offers advantages of high smoothness, driving comfort, and ease of construction, and is widely used in global road construction [1]. During long-term service, multiple challenges including traffic loading, temperature variations, ultraviolet radiation, and oxygen erosion lead to asphalt aging and hardening, resulting in micro-cracks [2, 3]. If these micro-cracks are not repaired in time, they gradually expand into macro-cracks, seriously compromising pavement structural integrity and durability, shortening service life, and increasing maintenance costs. Traditional repair methods such as surface spraying of rejuvenators suffer from poor penetration into pavement interior, limited repair effectiveness, and potential adverse effects on skid resistance, failing to meet practical engineering demands

*mafww1971@outlook.com

<https://doi.org/10.65102/is20261258>

for efficient self-healing technology [4]. Fatigue cracking arises from the combined effects of multiple factors, including material properties, environmental conditions, and traffic loading. Road researchers hope to elucidate the formation mechanisms and influencing factors of damage self-healing in asphalt materials, and identify appropriate methods to enhance the self-healing capability of asphalt materials to resist fatigue cracking and extend the service life of asphalt pavements [5, 6].

Zheng S et al. conducted fracture tests by constructing a model simulating the fracture process in temperature-sensitive hydrogels, validating the model against published experimental data on temperature-sensitive hydrogels from the literature. The tests revealed that this model is capable of simulating fracture processes for different types of temperature-sensitive hydrogels under various boundary conditions without requiring pre-existing cracks [7]. Pan Z et al. proposed a temperature-sensitive hydrogel in their article; after modification with sewage sludge ash (SSA), the modified hydrogel was tested, and results showed that FO-SSA-TSH achieved efficient pollutant removal across different Cr(VI) concentrations (0-40 mg/L), attributed to the high rejection rate of its FO membrane and the remarkable adsorption capacity of the hydrogel [8]. Feng J et al. proposed that self-healing capsules represent one of the most advanced methods in asphalt pavement preventive maintenance; whereas original designs had numerous limitations in mechanical performance and self-healing characteristics, Feng J et al. designed self-healing capsules with high microwave responsiveness for asphalt pavement. Through dynamic MRI tracking, microwave healing efficiency on asphalt pavement exceeded 90% within 30 seconds, with road performance surpassing conventional capsule systems [9]. Ding X et al. investigated the stress state of self-healing microcapsules during asphalt pavement service, establishing macroscopic structural models of asphalt pavement and multiscale models incorporating representative volume elements (RVE) containing self-healing microcapsules. Experiments found that increasing microcapsule content initially raised maximum principal stress and shear stress in capsule walls, but subsequently reduced these stresses [10]. MacCulloch K et al. proposed enhancing nuclear magnetic resonance (NMR) and magnetic resonance imaging (MRI) signals through reversible exchange signal amplification; after nearly 15 years of technical development in rat in vivo imaging and metabolic tracking studies, SABRE hyperpolarization chemistry was successfully translated to preclinical in vivo metabolic research. With advantages of low cost and easy operation, SABRE can be coupled with portable low-field NMR, breaking through traditional imaging sensitivity limitations and providing a novel technical pathway for MRI tracking signals [11].

The temperature-sensitive hydrogel self-healing asphalt concrete technology proposed in this study offers a new pathway for addressing these challenges, with the core principle being autonomous crack repair through energy supplementation. Temperature-sensitive hydrogels are a class of intelligent polymer materials responsive to temperature stimuli, with both hydrophilic and hydrophobic groups present on their molecular chains. The temperature-responsive characteristics of temperature-sensitive hydrogels can be adapted to the temperature variation patterns of asphalt pavements, enabling efficient release of healing agents under summer high temperatures or heat generated by vehicle loading to specifically repair cracks caused by temperature stress or loading.

2 Materials and Methods

This study selected SK-70 base asphalt as the matrix material. Performance indicators were tested according to the "Standard Test Methods for Bitumen and Bituminous Mixtures for

Highway Engineering." The penetration was 65.2 dmm at 25°C, 100 g, 5 s; the softening point was 48.5°C; and the ductility was 42.3 cm at 10°C, 5 cm/min.

The temperature-sensitive hydrogel used in this study was N-isopropylacrylamide-based hydrogel, synthesized by free radical polymerization [12]. N-isopropylacrylamide monomer, crosslinker N,N'-methylenebisacrylamide, initiator ammonium persulfate, and accelerator tetramethylethylenediamine were dissolved in deionized water in proportion, and reacted at 25°C for 24 h under nitrogen protection. After gel formation, the product was purified and dried. By regulating the dosage of crosslinker MBA, the hydrogel was prepared. The key parameters of the hydrogel were: lower critical solution temperature of approximately 33°C, crosslinking degree of 0.45%, and particle size distribution range of 50-80 µm.

The base asphalt was heated to 150±5°C to ensure flow state, and temperature-sensitive hydrogel particles were added at 5% of the asphalt mass. High-speed shear mixing was performed using a high-speed shear machine, with a shear rate of 5000 rpm, shear temperature of 160±5°C, and shear time of 40 minutes. After shearing, the modified asphalt was placed in an oven at 150°C for 30 minutes to eliminate bubbles, and then set aside for later use.

To meet the requirements of magnetic resonance imaging (MRI) for sample size and stability, the prepared temperature-sensitive hydrogel modified asphalt was injected into a custom polytetrafluoroethylene mold to produce cylindrical specimens with diameter of 10 mm and height of 15 mm. To ensure stable signal and no deformation of samples during testing, all samples were allowed to stand at room temperature of 25°C for 24 hours before testing to release internal stress.

To simulate micro-cracks generated in asphalt pavement during service, controllable micro-cracks were introduced inside the samples [13, 14]. A metal microneedle with diameter of 0.5 mm was inserted into the sample center along the axial direction at a rate of 0.1 mm/s to a depth of 10 mm, held for 5 seconds, and then slowly withdrawn, thereby forming uniformly sized, position-controllable micro-crack damage inside the sample [15, 16].

MRI experiments were conducted using a Bruker BioSpec 7.0T magnetic resonance imaging system, equipped with a 20 mm volume coil to match the sample size. A multi-echo spin echo sequence was employed to acquire T2-weighted images and T2 relaxation time spectra.

The main parameters were: repetition time = 3000 ms; echo time = 12 ms; field of view = 12 mm × 12 mm; image matrix = 256 × 256; slice thickness = 1.0 mm; slice gap = 0 mm; single scan time was approximately 3 minutes.

To achieve dynamic tracking of the temperature-triggered self-healing process, an in situ variable temperature module was used to control sample temperature. The first MRI scan was performed on pre-damaged samples at 20°C to record initial crack morphology. The sample chamber temperature was rapidly raised to 40°C to trigger hydrogel phase transition and initiate the self-healing process. Under constant temperature of 40°C, MRI scans were performed every 15 minutes, with total observation duration of 8 hours, to capture the complete dynamic process from crack formation to healing.

ParaVision 360 and ImageJ software were used for image post-processing and analysis. On T2-weighted images, regions containing crack areas were selected for signal intensity measurement. Three regions of interest (ROI) with area of approximately 2 mm² were selected at the center crack, and undamaged regions far from the crack were selected as reference ROI.

The relative signal intensity ratio (RSIR) was defined as $RSIR = SI_{\text{crack region}} / SI_{\text{reference region}}$. Higher RSIR values indicate stronger proton mobility in the crack region, usually corresponding to more complete gel filling and better healing performance. T2

relaxation time spectra were used to analyze the crack region, with T2 values plotted against time to track their evolution [17, 18].

To verify the reliability of MRI results, another batch of samples was prepared under identical preparation and damage conditions for conventional performance testing as control: using an Anton Paar MCR 302 dynamic shear rheometer in temperature sweep mode (20°C to 60°C), the complex modulus (G^*) and phase angle (δ) of modified asphalt and base asphalt were tested to evaluate the effect of hydrogel on asphalt viscoelasticity [19-21].

Three-point bending tests were conducted using a universal testing machine to load pre-damaged modified asphalt beam specimens (40 mm × 10 mm × 10 mm). The first loading was performed until specimen failure (generation of micro-cracks). After unloading, specimens were healed at 40°C for different durations (0 h, 2 h, 4 h, 8 h), and then reloaded until fracture. The self-healing efficiency (η) = (fracture energy of healed specimen / fracture energy of original specimen) × 100% was used as the evaluation index for macroscopic self-healing performance [22, 23].

Each time, $W_{d0} = 20\text{mg}$ dry hydrogel was weighed and placed in 50 mL deionized water, allowed to stand for 2 h at a rotation speed of 80 r/min, then the swollen hydrogel was removed with a colander and its mass (W) was weighed:

$$S = \frac{W_w - W_d}{W_d} \times 100\% \quad (1)$$

where S is the hydrogel swelling ratio, %; W_d is the dry hydrogel mass, mg; and W_w is the hydrogel mass after swelling, mg.

3 Results and Discussion

During the self-healing process of temperature-sensitive hydrogel modified asphalt triggered at 40°C, T2-weighted MRI images of the crack region at different healing times are shown in Figure 1. Representative images at five time points were selected: 0 min, 120 min, 240 min, 360 min, and 480 min. At the initial state (0 min), a low-signal dark region appeared in the crack area, indicating low proton density and restricted water molecule mobility in this region. When the healing time extended to 30 min, signal enhancement appeared at the crack edges, as the temperature-sensitive hydrogel underwent volume change when above LCST, expelling water molecules while the gel network filled the crack interior. At 120 min, signal enhancement occurred in the crack region, during which period the gel extensively filled the crack, forming continuous proton exchange. After 240 min, the signal intensity in the crack region stabilized, and the signal difference from the surrounding matrix asphalt gradually disappeared. By 480 min, the crack was no longer identifiable on MRI images, indicating that the micro-crack had achieved healing.

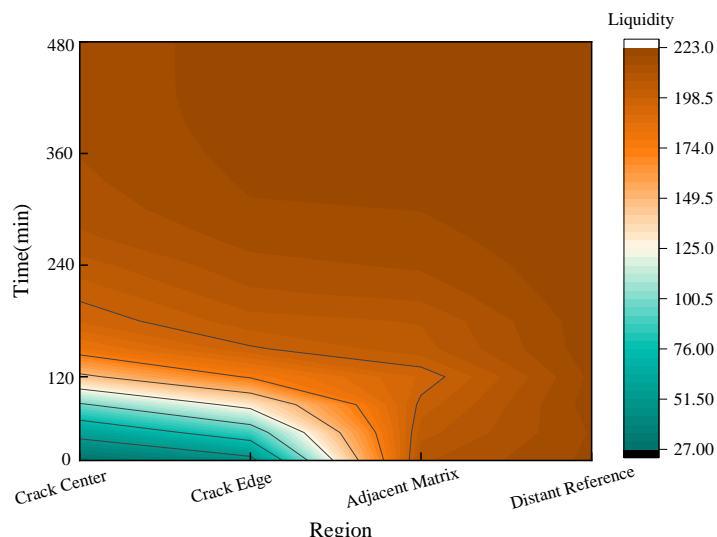


Figure 1: T2-weighted MRI images of the crack region at different healing times

Ratio analysis was performed on the signal intensity of the crack region ROI and reference region ROI to obtain the RSIR variation curve with healing time. Figure 2 shows the relative signal intensity ratio (RSIR) as a function of healing time.

In the first stage from 0 to 30 minutes, RSIR rapidly increased from the initial 0.32 to 0.68, with the maximum curve slope. This stage corresponds to rapid hydrogel phase transition and initial filling of the crack region. The second stage lasted from 30 to 240 minutes, with RSIR slowly increasing to 0.91 and the rising rate significantly slowing down. This indicates that the main crack space was essentially filled, with remaining pores being narrow, and the gel filling process gradually became limited by diffusion effects. The third stage extended from 240 minutes to 480 minutes, with RSIR stably maintained in the range of 0.92~0.95, showing no statistically significant difference compared to the reference region set at 1.0 ($p > 0.05$), marking the substantial completion of the specimen self-healing process.

The final RSIR failed to reach exactly 1.0, primarily because microscopic voids still remained inside the material, and proton exchange was restricted at the hydrogel-asphalt matrix interface. This also corresponds consistently with the characteristics of actually measured macroscopic self-healing efficiency.

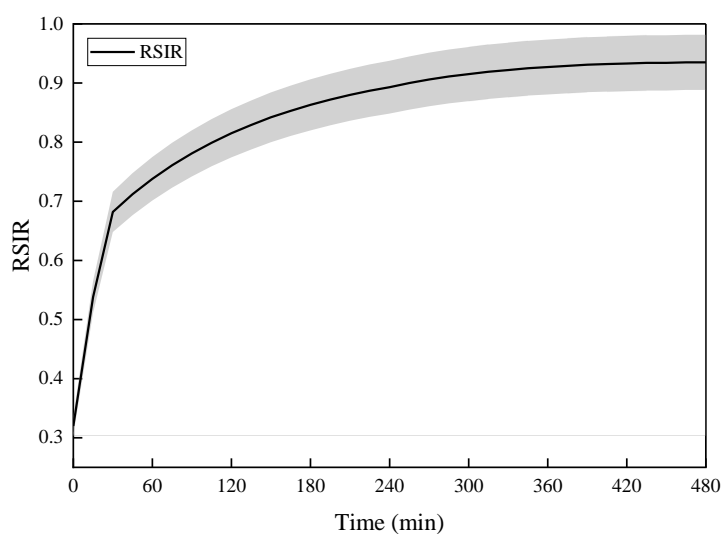


Figure 2: Relative Signal Intensity Ratio (RSIR) changes with healing time

T2 relaxation time is extremely sensitive to the motional environment and restricted state of water molecules. We obtained T2 relaxation time spectra through inversion of multi-echo MESE sequences to analyze the microscopic environmental changes in the crack region during the healing process. The evolution of T2 relaxation time spectrum in the crack region with healing time is shown in Figure 3. The T2 peak shifted from approximately 15 ms at 0 min to 8 ms at 120 min, and further to 7 ms at 480 min, indicating progressively restricted proton mobility associated with gel filling.

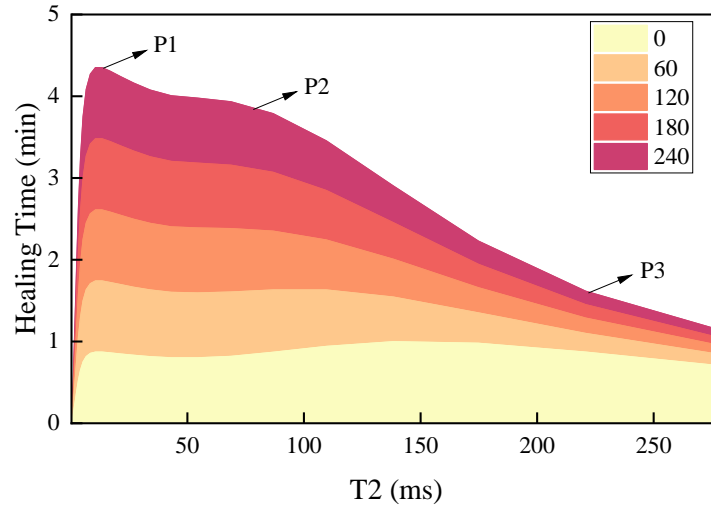


Figure 3: Evolution of T2 relaxation time spectrum in the crack region with healing time

Self-healing efficiency at different healing times is shown in Figure 4. It can be seen that self-healing efficiency η gradually improves with extended curing and healing time: 38.5% at 2 h healing, 67.2% at 4 h, and 89.3% at 8 h curing. This recovery pattern of macroscopic mechanical properties is consistent with the RSIR evolution characteristics measured by MRI in Figure 2, confirming that MRI technology can effectively track the entire self-healing process of temperature-sensitive hydrogel modified asphalt. Comparing the embedded stress-strain curves, after 8 h of healing and curing, fracture toughness and fracture energy recovered to levels of original specimens, indicating that temperature-sensitive hydrogel modified asphalt possesses excellent self-healing performance.

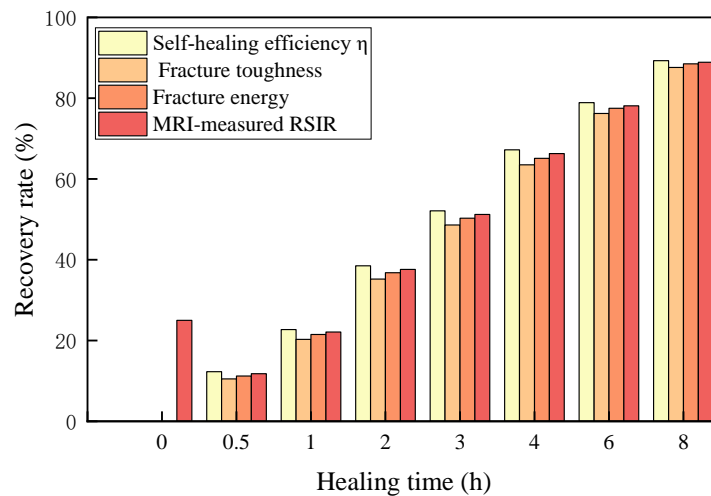


Figure 4: Self-healing efficiency (η) at different healing times

Temperature sweep rheological curves of base asphalt and temperature-sensitive hydrogel modified asphalt are shown in Figure 5. Figure 5(a) shows complex modulus G^* as a function of temperature. Throughout the tested temperature range, the complex shear modulus G of modified asphalt was consistently higher than that of base asphalt, with obvious differences in the 20~35°C interval. After incorporation of hydrogel particles, the asphalt's ability to resist high-temperature deformation was significantly enhanced. At approximately 33°C, the LCST phase transition temperature of the hydrogel, the G^* curve of modified asphalt exhibited a distinct inflection point, with the modulus decline rate slowing down. This is a direct manifestation of the temperature-sensitive hydrogel undergoing phase transition and regulating the rheological performance of the asphalt matrix. Figure 5(b) shows phase angle δ as a function of temperature, confirming that modified asphalt remains in a stable state in the 30~38°C interval around LCST. This change reflects the material characteristic transformation and is closely related to the continuously enhanced interfacial interaction when the temperature-sensitive hydrogel transitions from swollen to collapsed state.

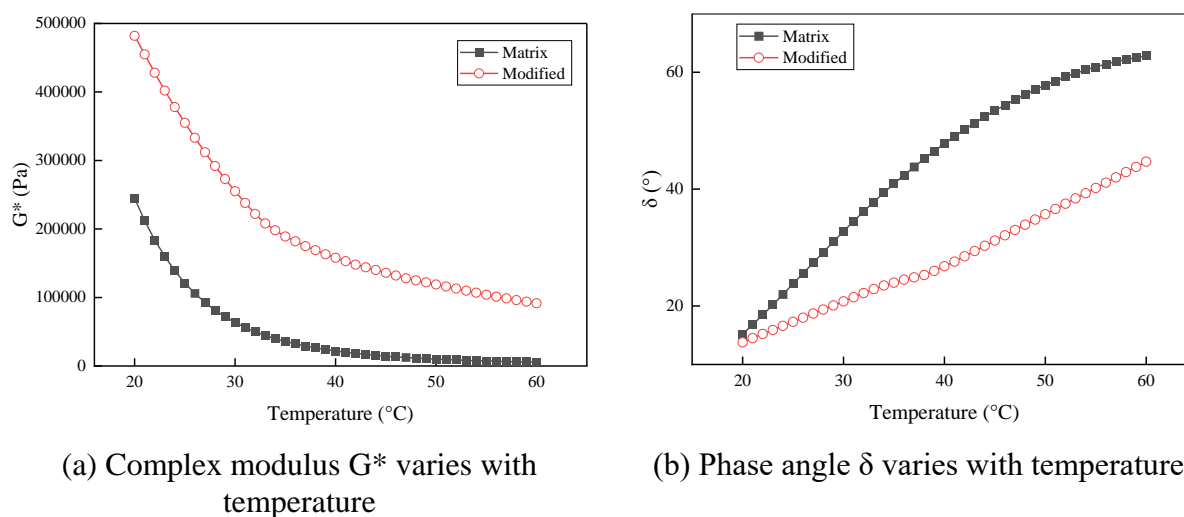


Figure 5: Temperature sweep rheological curves of base asphalt and temperature-sensitive hydrogel modified asphalt

The N-isopropylacrylamide-based temperature-sensitive hydrogel exhibited good adsorption performance for U(VI) in solution, with both adsorption capacity and removal rate reaching relatively optimal levels. The deviation in parallel experimental data was small, indicating stable adsorption performance of the temperature-sensitive hydrogel.

The adsorption rate is shown in Figure 6. The molecular chains of the N-isopropylacrylamide-based temperature-sensitive hydrogel possess both hydrophilic and hydrophobic groups, and the gel network structure contains numerous pores and active adsorption sites. It can bind with U(VI) ions through complexation, electrostatic adsorption, and other mechanisms, achieving efficient adsorption of target ions. The adsorption capacity stabilized at 6.5–36.9 mg/g within 90–120 min, demonstrating excellent adsorption kinetic characteristics and relatively fast adsorption rate of this temperature-sensitive hydrogel.

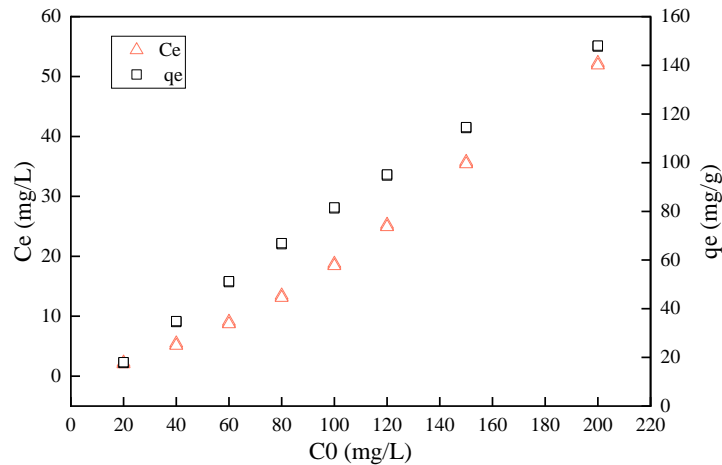


Figure 6: Adsorption rate

This adsorption performance reflects the structural advantages of the temperature-sensitive hydrogel itself, providing auxiliary support for its application in the modified asphalt system. The adsorption characteristics of the temperature-sensitive hydrogel enable it to interact better with asphalt molecules in the asphalt matrix, enhancing interfacial bonding force and reducing phase separation between the temperature-sensitive hydrogel and asphalt. The adsorption capacity for small molecules can also adsorb certain small molecular products generated during the asphalt aging process to some extent, thereby delaying the asphalt aging process.

Combined with MRI microscopic observation and macroscopic performance test results, the complete self-healing mechanism of temperature-sensitive hydrogel modified asphalt is elucidated [24, 25]. When the environmental temperature is below the LCST phase transition temperature, the hydrogel remains in a swollen state, forming a physical structure with the asphalt matrix. At this stage, even if micro-cracks are generated, the hydrogel cannot actively fill the gaps. Once the temperature rises above LCST, the temperature-sensitive hydrogel undergoes a volume phase transition, rapidly dehydrates and contracts, while simultaneously driving gel components to migrate and fill the crack interior, completing in situ repair of micro-cracks. By utilizing MRI technology to track proton mobility characteristics, the dynamic evolution patterns of the entire self-healing process can be intuitively observed, providing solid and reliable microscopic experimental support for subsequent optimization of self-healing asphalt formulations and improvement of material design concepts [26-28]. Specifically, we now state that the demonstrated adsorption capability reflects the hydrogel's high specific surface area and active sites, which may enhance interfacial bonding with the asphalt matrix and reduce phase separation.

4 Conclusion

In this study, temperature-sensitive hydrogel-modified asphalt was successfully prepared, and its self-healing law and action mechanism were elucidated by magnetic resonance imaging (MRI) dynamic tracking and macroscopic performance testing, and detailed and reliable experimental conclusions were obtained. The prepared N-isopropylacrylamide-based hydrogel had an LCST of approximately 33°C, crosslinking degree of 0.45%, and particle size of 50~80 micrometers. The modified asphalt prepared with 5% dosage could efficiently trigger self-healing at 40°C. The 5% dosage (by mass of asphalt) was determined based on preliminary experiments comparing 3%, 5%, and 7% incorporation levels, where 5% offered

the best balance of self-healing efficiency and rheological workability. MRI monitoring showed that the healing process divided into three stages: rapid RSIR increase from 0~30 min, slow growth from 30~240 min, and stabilization from 240~480 min. At 480 min, cracks became unidentifiable in images, indicating completion of microscopic healing. After 8 h of healing, the self-healing efficiency reached 89.3%, with fracture toughness and fracture energy approaching levels of original specimens. Rheological performance indicated that addition of temperature-sensitive hydrogel increased the complex modulus of asphalt, with the modulus change slowing at the 33°C phase transition point, enhancing high-temperature deformation resistance. The core mechanism of self-healing is that temperature-sensitive hydrogel dehydrates and contracts when temperature exceeds LCST, then migrates to fill cracks. MRI technology can precisely capture proton mobility and crack evolution characteristics, providing an effective means for microscopic characterization of self-healing asphalt. This technology enables in situ autonomous repair of micro-cracks in asphalt pavement, improving pavement durability and reducing maintenance costs, demonstrating good potential for engineering applications, and also providing experimental support and conceptual references for the design and performance evaluation of intelligent pavement materials.

About the Author

Yongjun Qiao, born in 1976 in Wudi County, Shandong Province, is a member of the Communist Party of China and holds a master's degree from Shandong University. Currently, he serves as an engineer at Shandong University Capital Operation Co., Ltd. Long-term committed to the research, development, and production of green, low-carbon, and high-performance road materials. qiao@sdu.edu.cn

Mingji Li, born in Juancheng County, Shandong Province in 1984, is a male member of the Communist Party of China and holds a bachelor's degree from Dezhou University. Currently, he serves as the General Manager of Shandong Huate Road Materials Co., Ltd. He has long been committed to the research, development, and production of green, low-carbon, and high-performance road materials. 285414826@qq.com

Fengwei Ma, born in 1971 in Wudi County, Shandong Province, is a member of the Communist Party of China and holds a master's degree. He currently serves as an Assistant Researcher at the Graduate School of Shandong University, responsible for graduate admissions and educational management. mafw1971@outlook.com

References

- [1] B. Bhatt and S. Wu, "A comprehensive state-of-art review on the use of rejuvenators in asphalt pavement," *J. Road Eng.*, vol. 5, no. 1, pp. 1–20, 2025. doi: 10.1016/j.jreng.2024.10.001
- [2] R. Mariyappan, J. S. Palammal, and S. Balu, "Sustainable use of reclaimed asphalt pavement (RAP) in pavement applications—a review," *Environ. Sci. Pollut. Res. Int.*, vol. 30, no. 16, pp. 45587–45606, Apr. 2023. doi: 10.1007/s11356-023-25847-3
- [3] A. Yousefi, A. Behnood, A. Nowruzi, and H. Haghshenas, "Performance evaluation of asphalt mixtures containing warm mix asphalt (WMA) additives and reclaimed asphalt pavement (RAP)," *Constr. Build. Mater.*, vol. 268, p. 121200, 2021. doi: 10.1016/j.conbuildmat.2020.121200

- [4] M. Hoy, V. Samrandee, W. Samrandee, A. Suddeepong, I. Phummiphan, S. Horpibulsuk, et al., "Evaluation of asphalt pavement maintenance using recycled asphalt pavement with asphalt binders," *Constr. Build. Mater.*, vol. 406, p. 133425, 2023. doi: 10.1016/j.conbuildmat.2023.133425
- [5] K. Zhao, W. Wang, and L. Wang, "Fatigue damage evolution and self-healing performance of asphalt materials under different influence factors and damage degrees," *Int. J. Fatigue*, vol. 171, p. 107577, 2023. doi: 10.1016/j.ijfatigue.2023.107577
- [6] C. Shi, R. Luo, H. Liu, and J. Yang, "Evaluation of self-healing characteristics of asphalt materials by intermittent loading tests," *Road Mater. Pavement Des.*, vol. 23, no. 11, pp. 2684–2696, 2022. doi: 10.1080/14680629.2021.1978525
- [7] S. Zheng, H. You, H. Li, and K. Y. Lam, "A model for fracture of temperature-sensitive hydrogel with diffusion and large deformation," *Eng. Fract. Mech.*, vol. 281, p. 109138, 2023. doi: 10.1016/j.engfracmech.2023.109138
- [8] Z. Pan, X. Yang, Y. Liang, M. Lyu, Y. Huang, H. Zhou, et al., "Chromium-containing wastewater reclamation via forward osmosis with sewage sludge ash temperature-sensitive hydrogel as draw agent," *J. Water Process Eng.*, vol. 51, p. 103422, 2023. doi: 10.1016/j.jwpe.2022.103422
- [9] J. Feng, Y. Song, S. Wu, Q. Zhang, Q. Liu, P. Wan, et al., "Microwave response mechanism and parameter optimization of microwave-responsive capsule (MRC) for asphalt pavement self-repairing," *Constr. Build. Mater.*, vol. 487, p. 142058, 2025. doi: 10.1016/j.conbuildmat.2025.142058
- [10] X. Ding, Y. Cui, T. Ma, and F. Ye, "Multiscale-mechanical analysis on self-healing microcapsules under asphalt pavement," *Constr. Build. Mater.*, vol. 443, p. 137670, 2024. doi: 10.1016/j.conbuildmat.2024.137670
- [11] K. MacCulloch, A. Browning, D. O. G. Bedoya, S. J. McBride, M. B. Abdulmojeed, C. Dedesma, et al., "Facile hyperpolarization chemistry for molecular imaging and metabolic tracking of [1-¹³C]pyruvate in vivo," *J. Magn. Reson. Open*, vol. 16-17, p. 100129, Dec. 2023. doi: 10.1016/j.jmro.2023.100129..
- [12] Y. Işıkver and D. Saraydın, "Smart hydrogels: Preparation, characterization, and determination of transition points of crosslinked N-isopropyl acrylamide/acrylamide/carboxylic acids polymers," *Gels*, vol. 7, no. 3, p. 113, Aug. 2021. doi: 10.3390/gels7030113.
- [13] J. Du, J. Wang, and Z. Fu, "Influence of interaction between microcracks and macrocracks on crack propagation of asphalt concrete," *Materials*, vol. 17, no. 12, p. 2877, Jun. 2024. doi: 10.3390/ma17122877.
- [14] A. Chen, G. D. Airey, N. Thom, Y. Li, and L. Wan, "Simulation of micro-crack initiation and propagation under repeated load in asphalt concrete using zero-thickness cohesive elements," *Constr. Build. Mater.*, vol. 342, p. 127934, 2022. doi: 10.1016/j.conbuildmat.2022.127934.
- [15] J. Du, X. Dai, Q. Liu, et al., "Toughening effect of micro-cracks on low-temperature

- crack propagation in asphalt concrete,” *Materials*, vol. 18, no. 11, p. 2429, 2025. doi: 10.3390/ma18112429.
- [16] S. I. Sarsam, “Influence of micro-crack healing on viscoelastic properties of moisture damaged asphalt concrete,” *Civil Engineering Beyond Limits*, vol. 3, no. 3, p. 1703, 2022. doi: 10.36937/cebel.2022.1703.
- [17] S. Guo, Z. Xu, X. Li, and P. Zhu, “Detection and characterization of cracks in highway pavement with the amplitude variation of GPR diffracted waves: Insights from forward modeling and field data,” *Remote Sens.*, vol. 14, no. 4, p. 976, 2022. doi: 10.3390/rs14040976.
- [18] H. Yuan, J. Ma, H. Ding, Y. Li, Y. Nie, Y. Qiu, et al., “Rheological, failure, and stress relaxation properties to control cracking in asphalt pavements,” *J. Mater. Civ. Eng.*, vol. 37, no. 9, p. 04025318, 2025. doi: 10.1061/JMCEE7.MTENG-20693.
- [19] Z. Zhao, F. Xiao, E. Toraldo, M. Crispino, and M. Ketabdari, “Effect of crumb rubber and reclaimed asphalt pavement on viscoelastic property of asphalt mixture,” *J. Clean. Prod.*, vol. 428, p. 139422, 2023. doi: 10.1016/j.jclepro.2023.139422.
- [20] T. Bai, X. Huang, X. Zheng, H. Wang, Y. Cheng, B. Cui, et al., “Viscoelastic parametric conversions and mechanical response analysis of asphalt mixtures,” *Constr. Build. Mater.*, vol. 390, p. 131777, 2023. doi: 10.1016/j.conbuildmat.2023.131777.
- [21] F. Autelitano, D. Petrolo, L. Chiapponi, F. Giuliani, and S. Longo, “Temporary clogging effects induced by a sustainable anti-icing hydrogel on the hydraulic conductivity and inertia coefficient of open-graded asphalt pavements,” *Constr. Build. Mater.*, vol. 361, p. 129495, 2022. doi: 10.1016/j.conbuildmat.2022.129495.
- [22] A. Seitllari, “Investigating the fatigue life of asphalt pavements under different aging levels using the three-point bending cylinder (3PBC) test and mechanistic-empirical analysis,” *Mater. Struct.*, vol. 58, no. 4, p. 124, 2025. doi: 10.1617/s11527-025-02659-0.
- [23] X. Zhang, E. Chen, P. Gao, and C. Si, “Microdynamic simulations of crack evolution in asphalt mixtures under three-point bending loads,” *Arch. Appl. Mech.*, vol. 91, no. 11, pp. 4485–4497, 2021. doi: 10.1007/s00419-021-02020-1.
- [24] A. Jalal and R. Kiran, “Sustainable biobased hydrogel as an alternative air-entrainment agent in cement-based materials,” *J. Mater. Civ. Eng.*, vol. 36, no. 11, p. 04024342, 2024. doi: 10.1061/JMCEE7.MTENG-17763.
- [25] H. Wang, L. He, and B. Tang, “Characterization of temperature regulating, high-temperature rheological and anti-aging properties of asphalt mastic modified with SSPCMs,” *Constr. Build. Mater.*, vol. 445, p. 137991, 2024. doi: 10.1016/j.conbuildmat.2024.137991.
- [26] W. Li and W. Chen, “Improving cement paste performance with temperature-sensitive PNIPAM hydrogel particles,” *Innov. Int. Multi-discip. J. Appl. Technol.*, vol. 2, no. 6, pp. 157–166, 2024.
- [27] H. Wang, Q. Liu, J. Wu, P. Wan, and F. Zhao, “Self-healing performance of asphalt

concrete with Ca-alginate capsules under low service temperature conditions,” *Polymers*, vol. 15, no. 1, p. 199, Dec. 2022. doi: 10.3390/polym15010199.

- [28] S. Wang, K. Wei, W. Shi, P. Cheng, J. Shi, and B. Ma, “Study on the rheological properties and phase-change temperature regulation of asphalt modified by high/low-temperature phase change material particles,” *J. Energy Storage*, vol. 56, p. 105970, 2022. doi: 10.1016/j.est.2022.105970.